unten her allseitig beleuchtet, ohne daß Strahlen direkt in das Objektiv gelangen. Der Objektträger T mit dem in einer Flüssigkeit darauf befindlichen Präparat muß dazu unter Zwischenschaltung von Wasser oder Zedernholzöl auf die obere Fläche des Kondensors aufgelegt werden. Die durch den Objektträger, das Präparat und das Deckglas D dringenden Strahlen werden an der Oberfläche des Deckglases total reflekteirt und treten bei A und B wieder aus. Die an den beleuchteten Teilchen des Präparates abgebeugten Wellen fallen z. T. unter kleineren Winkeln als dem Grenzwinkel der Totalreflexion auf die Oberfläche des Deckglases und treten durch dieses in die umgebende Luft und dann in das Objektiv aus. (In Abb. 3.92 sind diese Strahlen gestrichelt gezeichnet.)

**Phasenkontrastverfahren nach Zernike.** Als Modell eines im Mikroskop zu betrachtenden Objekts ist bisher ein Gitter betrachtet worden, weil sich alles Wesentliche der Abbeschen Theorie des Mikroskops daran erläutern ließ. Dieses Gitter bestand aus abwechselnd durchsichtigen und undurchsichtigen Teilen, die seine Struktur bildeten. Ein solches Gitter wird *Amplitudengitter* genannt, weil die Amplitude der hindurchtretenden Strahlung vom vollen Wert in den durchlässigen Teilen bis zum Wert Null in den undurchlässigen variiert. Objekte, die ihre Struktur durch die Verschiedenheit der hindurchgelassenen Lichtamplituden offenbaren, nennt man entsprechend *Amplitudenobjekte*. Es gibt aber auch, wie schon in Abschn. 3.10 erwähnt, strukturierte Objekte, die an allen Stellen völlig durchlässig sind; ihre Struktur ist darin begründet, daß infolge von lokalen Variationen der Brechzahl die Phasen der hindurchtretenden Lichtwellen nicht konstant sind – daher der Name *Phasenobjekte*, wofür als Beispiel eine Ultraschallwelle dienen mag, die ein ausgezeichnetes Phasengitter liefert. Phasenobjekte erzeugen im primären Bilde genau wie Amplitudenobjekte die ihrer Natur entsprechenden Beugungsspektren, aber man kann ihre Struktur ebensowenig mit einem Mikroskop wie mit dem Auge sehen, da dieses nicht die Fähigkeit besitzt, Phasenunterschiede zu erkennen. Der praktische Mikroskopiker hat sich bisher in diesem Falle dadurch geholfen, daß er die Objekte geeignet färbte und sie – so gut wie möglich – in Amplitudenobjekte umwandelte. Solche Färbemethoden haben z. B. in der Bakteriologie eine große Rolle gespielt. Natürlich bedeutet Färbung immer einen Eingriff in das Präparat, dessen Tragweite schwer abzuschätzen ist. Deshalb stellt es einen großen Fortschritt dar, daß es F. Zernike (1932) gelungen ist, auf rein optischem Wege (sog. **Phasenkontrastverfahren**) Phasenstrukturen ohne den geringsten Eingriff in das Präparat sichtbar zu machen.

Zur Erläuterung des Phasenkontrastverfahrens soll an die Abbesche Theorie angeschlossen werden und die Verteilung der gebeugten Intensität in der hinteren Brennebene des Objektivs für ein Amplituden- und Phasenobjekt verglichen werden. Der Zusammenhang zwischen Objekt und Beugungsbild ist nach Gl. (3.49) durch eine Fourier-Transformation gegeben, die hier in folgender Form geschrieben werden soll:

$$E(x,y) \sim \mathrm{Re}\, \mathrm{e}^{-\frac{2\pi i l}{\lambda}} \iint F(\xi,\eta)\, \mathrm{e}^{2\pi i \nu t}\, \mathrm{e}^{-\frac{2\pi \mathrm{i}}{\lambda f}(x\xi + y\eta)}\, \mathrm{d}\xi\, \mathrm{d}\eta\,. \tag{3.74}$$

Dabei kann der Ausdruck $\mathrm{Re}\, F(\xi,\eta)\, \mathrm{e}^{2\pi i \nu t}$ als elektrische Feldstärke unmittelbar hinter der Objektebene gedeutet werden. Bei einem Amplitudenobjekt ist $F(\xi,\eta)$ reell, und die Feldstärke besitzt in der Objektebene konstante Phase. Dies kommt dadurch

zustande, daß die Beleuchtungswelle vor der Objektebene mit $e^{2\pi i\nu t}$ angesetzt wurde, also eine örtlich konstante Phase besitzt. Die Feldstärke unmittelbar hinter der Objektebene ergibt sich durch Multiplikation der Beleuchtungswelle mit dem Schwächungsfaktor $F(\xi, \eta)$. Bei einem Phasenobjekt wird dagegen die Phase der ebenen Beleuchtungswelle örtlich um eine Phasengröße $\vartheta(\xi, \eta)$ variiert, so daß die Feldstärke hinter der Objektebene gegeben ist durch $e^{i2\pi\nu t - i\vartheta}$. Die Beugung an einem Phasenobjekt kann demnach ebenfalls mit Hilfe von Gl. (3.74) behandelt werden, wenn angesetzt wird

$$F(\xi, \eta) = e^{-i\vartheta(\xi, \eta)}. \tag{3.75}$$

Bei der weiteren Betrachtung sollen schwache Phasenobjekte angenommen werden, d. h. $\vartheta \ll 1$. Dann gilt näherungsweise

$$F(\xi, \eta) = 1 - i\vartheta(\xi, \eta). \tag{3.76}$$

Einsetzen in Gl. (3.74) ergibt unter Ausnutzung von $-i = e^{-\frac{i\pi}{2}}$

$$E_p(x, y) \sim \mathrm{Re}\, e^{-\frac{2\pi i l}{\lambda}} \iint e^{2\pi i\nu t} e^{-\frac{2\pi i}{\lambda f}(x\xi + y\eta)} d\xi d\eta$$
$$+ \mathrm{Re}\, e^{-\frac{2\pi i l}{\lambda} - \frac{i\pi}{2}} \iint \vartheta(\xi, \eta) e^{2\pi i\nu t} e^{-\frac{2\pi i}{\lambda f}(x\xi + y\eta)} d\xi d\eta. \tag{3.77}$$

Für die Beugung an einem schwachen Amplitudengitter mit $F(\xi, \eta) = e^{-k(\xi, \eta)} \approx 1 - k$, ergibt sich analog mit $-1 = e^{-i\pi}$:

$$E_A(x, y) \sim \mathrm{Re}\, e^{-\frac{2\pi i l}{\lambda}} \iint e^{2\pi i\nu t} e^{-\frac{2\pi i}{\lambda f}(x\xi + y\eta)} d\xi d\eta$$
$$+ \mathrm{Re}\, e^{-\frac{2\pi i l}{\lambda} - i\pi} \iint k(\xi, \eta) e^{2\pi i\nu t} e^{-\frac{2\pi i}{\lambda f}(x\xi + y\eta)} d\xi d\eta. \tag{3.78}$$

Die gebeugte Feldstärke $E_p(x, y)$ besteht nach vorstehenden Gleichungen aus zwei Summanden. Der erste Summand beschreibt die Beugung an einem Objekt mit konstantem Transmissionsgrad 1. Dies ergibt gar keine Beugung, sondern eine ungeschwächt durch das Objekt tretende Welle. Der zweite Summand beschreibt die eigentliche Beugung. Er ist beim Amplitudengitter und Phasengitter ähnlich aufgebaut. Der einzige Unterschied ist, daß beim Phasengitter in der gebeugten Intensität gegenüber dem Amplitudengitter eine Phasenverschiebung von $\pi/2$ auftritt.

Dies macht tatsächlich den Unterschied in der mikroskopischen Abbildung von Amplituden- und Phasenstrukturen aus; man muß sich ja klar machen, daß das sekundäre Bild im Sinne Abbes, d. h. das Abbild des Objektes, eine *Interferenzerscheinung* ist, die von den Spektren des primären Bildes erzeugt wird: Daß dabei Phasendifferenzen die entscheidende Rolle spielen, ist also selbstverständlich. Damit aber hat man schon den Grundgedanken des Zernike-Verfahrens: Man hat nur die Phase im Zentralbild des Phasenobjektes um $\pi/2$ zu ändern, um den Unterschied zwischen Amplituden- und Phasenobjekten zum Verschwinden zu bringen, d. h. Phasenstrukturen genau wie Amplitudenstrukturen erkennbar zu machen.

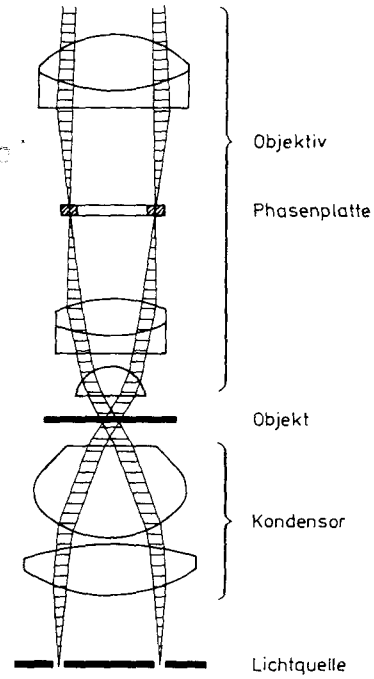


**Abb. 3.93** Strahlenverlauf in einem Phasenkontrastmikroskop.

Die Lösung dieser Aufgabe gelang Zernike dadurch, daß er in den Gang der Strahlen, die das Zentralbild erzeugen, in der Brennebene des Mikroskopobjektivs eine *Phasenplatte* einschaltete, die dem durchtretenden Licht eine Phasenverschiebung von $\pi/2$, also einem Gangunterschied von $\lambda/4$, aufprägt. In der Praxis wird diese Phasenplatte zweckmäßiger durch eine ringförmig auf eine Glasplatte aufgedampfte, $\lambda/4(n-1)$ dicke Schicht einer geeigneten Substanz hergestellt. Ein solcher Phasenring setzt voraus, daß das zur Beleuchtung dienende Licht von einer ringförmigen Lichtquelle herkommt. Man erreicht dies z. B. durch eine vor dem Mikroskopkondensor angebrachte ringförmige Blende, wie in Abb. 3.93 dargestellt. In Abb. 3.93 sind nur Strahlen gezeichnet, die dem Zentralbild entsprechen. Die das Objekt abbildenden, abgebeugten Strahlen sind weggelassen.

Da das beim Phasenkontrastverfahren in die höheren Ordnungen abgebeugte Licht schwächer ist als das ungebeugte, das durch die Phasenplatte geht, gibt man letzterer eine kleine zusätzliche Absorption; denn man erhält bei einer Interferenzerscheinung besonders große Helligkeitsunterschiede und somit kontrastreichere Bilder, wenn (neben der richtigen Phasenbeziehung) die miteinander interferierenden Lichtbündel gleiche Amplituden haben.

In Abb. 3.94 ist das 378fach vergrößerte Bild eines ungefärbten Schnittes durch eine Rattenniere im gewöhnlichen Hellfeld (a) und im Phasenkontrastverfahren (b) wiedergegeben. Wie man sofort sieht, kommen im letzteren Fall Zellmembran, Zellkern, Nukleoli und vieles andere, was im Helfeld nur angedeutet ist, klar heraus.

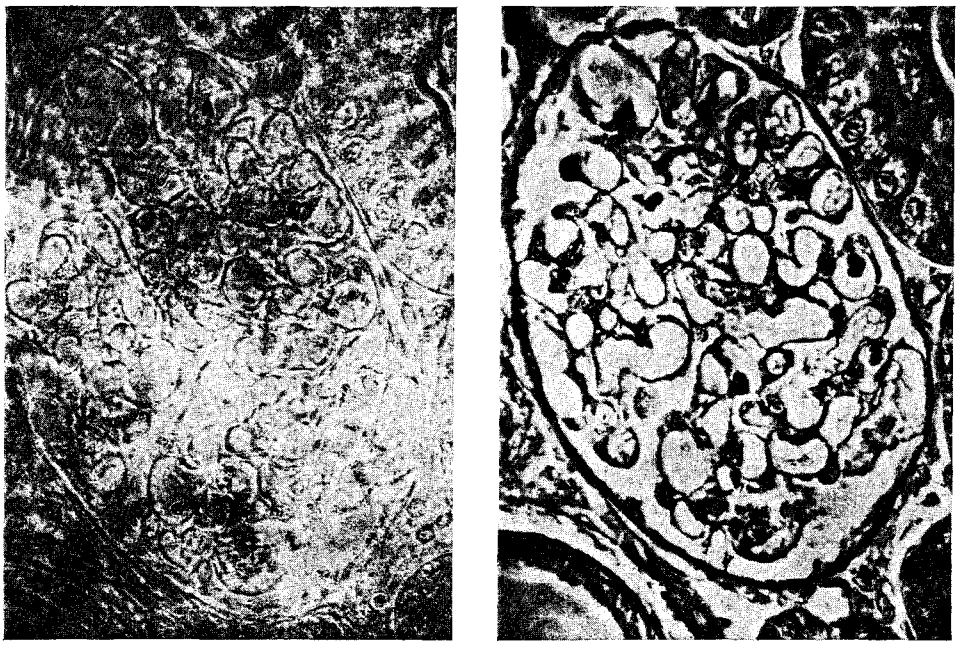

a) b)

**Abb. 3.94** a) Hellfeld und b) Phasenkontrast-Mikroaufnahme eines ungefärbten Schnittes durch eine Rattenniere; Vergrößerung 378fach.

Sowohl die Dunkelfeldanordnung als auch das Phasenkontrastverfahren kann man mit der gleichen Anordnung demonstrieren, mit der man die Abbesche Theorie der Abbildung von Nichtselbstleuchtern im Vorlesungsversuch vorführt (vgl. Ausführungen zu Abb. 3.88). Statt der spaltförmigen Öffnung in einem undurchsichtigen Schirm an der Stelle des primären Bildes bringt man eine (völlig durchsichtige) Glasplatte an. Blendet man das Zentralbild der Lichtquelle durch ein dunkles Scheibchen geeigneter Größe auf der Glasplatte ab, so beobachtet man eine vorhandene Struktur des Objektes im Dunkelfeld. Bringt man statt dieses undurchsichtigen Scheibchens aber eine Phasenplatte an, so erkennt man die Phasenstruktur des Objektes mit Hilfe des Phasenkontrastverfahrens; man kann z. B. auf diese Weise ein durch Ultraschall erzeugtes Phasengitter wie ein Amplitudengitter abbilden.

**Schatten- und Schlierenmethode.** Die im vorhergehenden geschilderten Methoden zur Sichtbarmachung von Phasenstrukturen haben eine nahe Beziehung zu älteren Verfahren, gröbere Phasenstrukturen, sog. *Schlieren,* sichtbar zu machen; diese Verfahren werden auch heute noch vielfach benutzt, weswegen hier auf sie hingewiesen sei.

Das einfachste Verfahren ist die sog. *Schattenmethode,* mit deren Hilfe man Schlieren objektiv sichtbar machen kann. Man benutzt eine möglichst punktförmige Lichtquelle (Krater einer Bogenlampe) zur direkten Beleuchtung eines Projektionsschirmes; dieser ist vollkommen gleichmäßig erleuchtet, wenn die Lichtquelle nur voll-

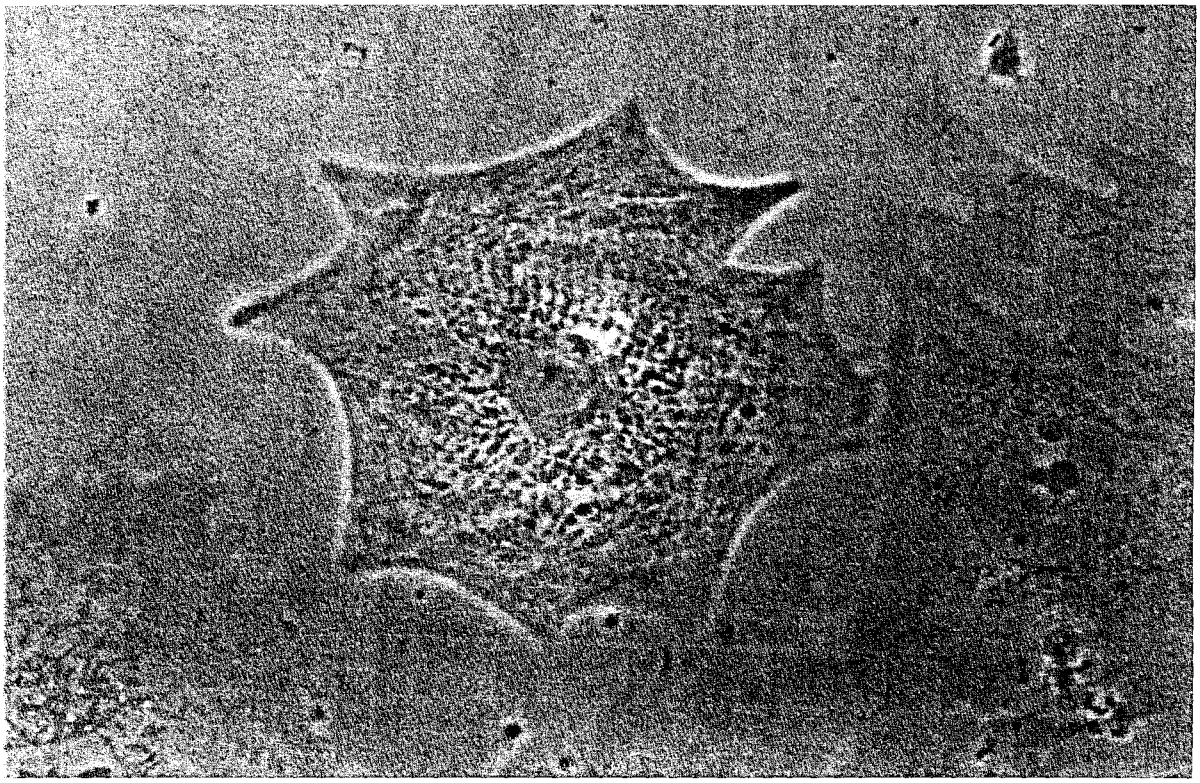

FIGURE 2 Living heart muscle cell in phase contrast (objective lens Plan-Neofluar 100×/1.3 oil Ph3).

ness differences are clearly visible to the human eye. For example, when light passes the relatively thick and dense cell nucleus, more light will be diffracted than by the nearby thin and nearly translucent cell cytoplasm. Therefore, in phase-contrast microscopy the nucleus will appear darker than the surrounding cytoplasm.

The adjustment of the phase-contrast setup is easy. The selected phase annulus in the condenser system should match the phase number of the objective lens. For example, the objective lens labeled Ph2 needs a phase ring with the number 2 in the condenser system. With the help of a centering telescope or, in some microscopes, inbuilt Bertrand optics, the bright annular illumination transmitted by the phase ring in the condenser and the dark phase annulus of the objective lens are made visible. The lateral position of the phase ring in the condenser is adjusted until it is concentric with and completely contained within the phase annulus of the objective lens. This procedure results in a properly set phase contrast. Changing to objective lenses with other phase rings (1 or 3) requires a change of the condenser phase ring as well with a check for its correct alignment.

### B. NOMARSKI (DIFFERENTIAL-INTERFERENCE) CONTRAST MICROSCOPY

As for phase contrast, the DIC technique in transmitted light also permits visualization of a flat unstained specimen, but with the addition of a three-dimensional "shadowcast" appearance (Fig. 3). The specimen can be somewhat thicker and have a greater difference in refractive indices than the phase-contrast specimen. The physical principles and operation of the DIC optics are totally different from those of phase contrast and are technically far more complicated.

FIGURE 3 Living cells of a brain section in Nomarski (differential-interference) contrast under infrared light observation (objective lens Achroplan 40×/0.75 W).

First, polarized light is used. In addition to the objective lens, four optical components are necessary to perform Nomarski (differential-interference) contrast: polarizer, DIC prism, DIC slider, and analyzer.

In the transmitted light path a polarizer is mounted directly in front of the condenser system, causing the light to be linearly polarized. In the condenser itself a cemented quartz Wollaston prism, or DIC prism, is placed. This prism splits each light wave into two waves with two different polarization vibration directions ($x$ and $y$), which diverge at a very small angle. The condenser optics aligns the two waves to both be parallel to the optical axis of the microscope. The lateral spacing of the two waves is in the order of magnitude of micrometers and does not exceed the limit of resolution. Thus no double image occurs in the eyepiece. The two light waves, which are initially identical in phase, are projected through adjacent regions of the specimen. The phase specimen now induces path differences at the two waves according to its thickness and refractive indices. A second Wollaston prism, the DIC slider, situated at (or near) the back focal plane of the objective, is used to recombine these two waves into a single beam. The two vibration planes ($x$ and $y$) still exist. At the end, the light beam passes a second polarizing element, the analyzer, which is mounted at right angles to the orientation of the polarizer before it forms the DIC image in the eyepiece. The analyzer transforms the two perpendicular waves into two waves with a common vibration plane, thereby enabling them to interfere. The path difference between the $x$ and $y$ waves is responsible for more or less transmitted light. A path difference with the value of 0 results in no transmitted light by the analyzer. Maximum light is transmitted if the path difference is half the

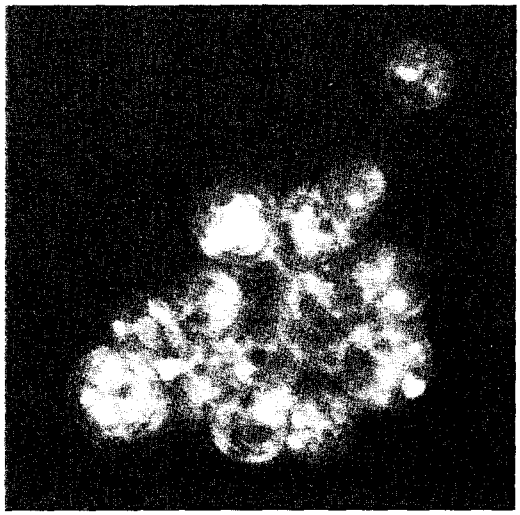

FIGURE 4 Plant protoplasts under dark-field observation (objective lens Achrostigmat 10×/0.25 Ph1).

wavelength. By these means, different regions of the specimen appear bright or less bright in contrast to the mid-grey of the background.

To modify and optimize the image contrast, the DIC slider, the second Wollaston prism in the light pathway, has a longitudinal fine adjustment to alter the path difference, which affects the brightness of the image. The setting of the DIC slider generates a positive or negative shadowcast appearance of the specimen details, one edge having a bright border and the opposite edge, a dark border. This gives an artifactual three-dimensional impression of the specimen.

A proper microscope setup for the DIC technique is achieved by first aligning all optical components according to the Köhler illumination rules. A second step is to check the correct crossed position of polarizer and analyzer without the DIC prism in the condenser, without the DIC slider in the objective nosepiece, and without the specimen: a dark image is the result. The Wollaston prisms are then inserted at 45° to its polarizer, and adjusted for optimal contrast. Note that the DIC sliders and prisms are specific for particular objective lenses. The numerical aperture indicated on the DIC elements has to match the numerical aperture of the objective lens.

### C. DARK-FIELD MICROSCOPY

In dark-field microscopy, the illuminated object appears bright against the black background (Fig. 4). By means of a large central opaque stop in the condenser, direct axial illumination of the specimen is prevented, the illuminating rays of light coming only from the side, at an angle that exceeds the collecting angle of the objective lens. As a consequence, only light scattered by parts of the object enters the objective lens. This results in an extraordinarily high contrast of the specimen. It is even possible to visualize particles in the specimen whose sizes are considerably smaller than the resolution of the microscope, although their shape cannot be detected.

The simplest optical configuration for dark-field microscopy uses a phase-contrast condenser together with a bright-field (non-Ph) objective lens. The annular stop of the condenser has to be larger than the exit pupil of the objective lens, for example, a Ph3 phase ring in the condenser and a 10×/0.3 objective lens. The specimen is then illuminated by a cone of light with an angle of the inner aperture larger than the

collecting aperture of the objective lens. Specimen areas with no specific structures or empty spaces appear dark. The scattered or diffracted light from the specimen enters the objective lens and forms the dark-field image.

Specific dark-field condenser systems are also available, with a numerical aperture higher than the numerical aperture of the objective lens used. To facilitate reduction of the observation aperture to below that of the annular illumination, objective lenses with an inbuilt iris diaphragm are recommended.

Setting up Köhler illumination for dark-field microscopy is a little more difficult and tricky than for bright-field illumination because of the low imaging quality of these condensers. Only practice and the advice of an already experienced person solve this problem. As only scattered light is detected by the objective lens, all optical surfaces, especially the condenser front lens, the specimen, and the objective front lens, must be extremely clean. Dirty surfaces produce additional scattered light which does not come from the specimen but just increases the brightness of the image background. For an optimum dark-field image, the condenser aperture and field diaphragm of the transmitted light path must be fully open.

## D. BLACK AND WHITE AND COLOR PHOTOMICROGRAPHY

For photomicrographic documentation the light microscope has to be equipped with optical exits offering a defined intermediate image plane where camera systems can be attached. Two camera types are available to take micrographs from the specimen. One type is represented by the well-known reflex cameras from various manufacturers, which include all necessary elements like shutter and light measurement device for the calculation of exposure time. In many microscopes reflex cameras can be mounted directly on the microscope stand via so-called T-adapters. In others, additional optical components are required to project the intermediate image to the film plane, for which technical advice should be sought from a representative of the microscope manufacturer. The second type of camera is exemplified by the specialized microscope camera systems produced by microscope manufacturers. Besides attachable camera systems, there are true photomicroscopes with all the necessary camera elements to generate micrographs of the specimen built in.

The main differences between reflex cameras, microscope camera systems, and photomicroscopes are flexibility and performance. Most reflex cameras offer automatic exposure only up to around half a minute, which requires a lot of battery energy. Not all reflex cameras allow the operator to expose several times onto the same image to perform multiple exposures after double- or triple-staining procedures. Microscope camera systems and photomicroscopes offer features including automatic exposure time determinations with integral and point measurement, serial exposure with different exposure times, Schwarzschild effect compensation, and PC control via interfaces.

For all photomicrographic systems two filters are important: an interference green filter for black and white photography and a conversion filter (3200–5500°K) for color photography. In black and white photomicrography the green filter gives a slightly increased contrast in the image. The conversion filter is used to vary the color temperature of the light source to a higher temperature to allow daylight color film to be used in color micrography without color changes in the photographed specimen. In addition, neutral density filters to attenuate light intensities and color-compensating filters to avoid color distortion (Schwarzschild effect) at long-duration exposures may be necessary.

Today, nearly any film material can be used without significant limitation. The image resolution and brilliance of the photograph are, to a certain extent, related to the film speed. High-speed film material shows a little more grain structure and, therefore, a weaker image compared with the sharp and crisp images of low-speed

# Reflection Interference Microscopy

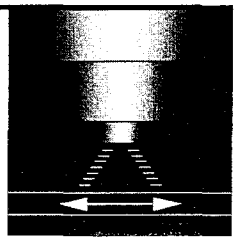

Jürgen Bereiter-Hahn and Pavel Vesely

## I. Introduction

Reflection microscope arrangements are extensively used to study surface topography of opaque objects and of specimens transmitting light. The resolution in $z$ axis of these methods by far exceeds the lateral resolution of a light microscope, reaching the nanometer range. The *relative reflectivity* (RI), defined as the ratio of photon fluxes reflected from the object and from the background depends on the differences in refractive indices of the media forming a boundary. The reflectivity $R$ (fraction of incident light intensity that is reflected at a boundary) of one optical interface is described for homogeneous, absorption-free, transparent and isotropic media by the Fresnel equations:

For normal incidence,

$$R_0 = \left(\frac{n_0 - n_1}{n_0 + n_1}\right)^2 \tag{1}$$

In the case of reflection at an optically denser medium ($n_1 > n_0$), a phase shift of $\pi$ results for the reflected *amplitude* $r$ (the calculated value of intensity $R$ corresponds to the product of an amplitude and its conjugated complex value $\bar{r}$).

For oblique incidence, reflection depends on the relative orientation of the reflecting plane and the polarization plane of the incident light:

$$R_\perp = + \frac{\sin^2(\varphi_0 - \varphi_1)}{\sin^2(\varphi_0 + \varphi_1)} \tag{2}$$

$$R_\parallel = + \frac{\tan^2(\varphi_0 - \varphi_1)}{\tan^2(\varphi_0 + \varphi_1)} \tag{3}$$

with

$\varphi_0$ = angle of incidence
$\varphi_1 = \arcsin[(n_0/n_1)\sin \varphi_0]$ = angle of refraction as a function of the angle of incidence dependent on the adjacent refractive indices
$R_\perp$, $R_\parallel$ = reflectivity referring to vertical and parallel polarized light, respectively.

At angles of incidence $\varphi_0 \leq 25°$ (under some conditions even more) the simple Fresnel equation for normal incidence can be used without causing major errors in the calculation of reflectivity. If reflectivity calculations are based on RI the error introduced by this simplification is diminished.

Living as well as fixed cells attached to a plain surface can be investigated using reflection-type microscopes. The resulting image is determined by the RI at different areas of the cell and by interferences of the light reflected at different boundaries

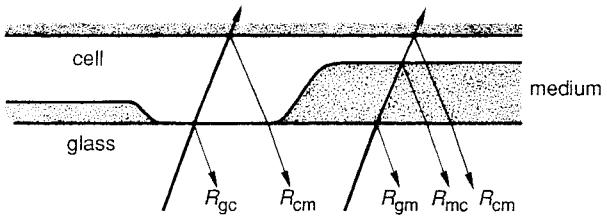


FIGURE 1 Schematic representation of the main reflecting interfaces in a cell preparation on a cover glass. The thick arrows indicate the incident beams; the thin arrows, the reflected beams with the relative intensity $R$. The suffixes indicate the optical media forming the interface. The phase of $R_{mc}$ is shifted for $\lambda/2$ at the reflecting surface. (Reproduced, with permission from Bereiter-Hahn *et al.* (1979).)

(Fig. 1). Considering the dominance of interferences, microscope arrangements visualizing the reflections delineated in Fig. 1 have been termed interference reflection microscopy (IRM), reflection interference microscopy (RIM), reflection interference contrast microscopy (RIC), or reflection contrast microscopy (RCM). To us RIM seems to be the logically most convincing term and correctly emphasizes the fact that this type of interference microscopy is based on light *reflections*. It is a more general term than RIC which, in addition, denominates the fact that in some cases contrast-enhancing precautions are taken (i.e., presence of a ring-shaped diaphragm). Therefore these two terms will be used throughout this description.

The technical difficulties in RIM arise from the very small differences in the refractive index of cytoplasm and the surrounding medium. The reflections at cell surfaces are in the range of about 0.4% of the incident light. Therefore, high intensities of illumination and/or very sensitive recording devices have to be used. Furthermore, RIM images are sensitive to unwanted reflections in the optical system. The principle dates back to the surface contact microscope described by Ambrose (1956), who coupled a glass slide with cells to a 60° prism and illuminated the upper surface of the glass slide at an angle greater than the critical angle. Thus, the light is totally internally reflected at the glass/water interface. At those zones of cells that make close contact with the surface of the glass, the difference in refractive indices is smaller, thus allowing the beam to evanesce from the glass surface into the cytoplasm. The light may be scattered and enter the objective lens which was positioned above the cell. In this case the image field appears completely dark at all clean and cell-free areas (due to total reflection), whereas regions where cells adhere closely to the glass are brightly illuminated.

Curtis (1964), also using an upright microscope stage and almost normal incidence of the intensely collimated illuminating light beam, termed this technique *interference reflection microscopy*. Ploem (1975) combined epi-illumination through the objective lens and the use of polarized light, a Stach's stop (ring-shaped illuminating aperture), and a rotatable quarter wavelength plate. The polarizing system was designed to exclude light reflected in the optical system (see legend to Fig. 2); Stach's aperture allows conical illumination of the specimen and thus increases the contrast of fine surface structures (oblique illumination). In addition, this aperture allows illumination at a known and defined angle of incidence (corresponding to a certain range of the illuminating numerical aperture).

## II. Materials and Instrumentation

### A. GENERAL ARRANGEMENTS

RIM can be performed with any microscope stage, upright or inverted. The specific requirements are an analyzer and epi-illumination equipment, including a strong

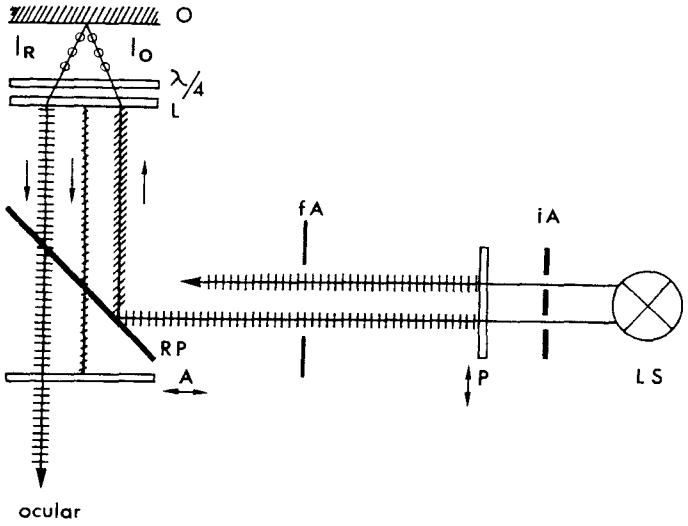


FIGURE 2 Diagram of the Leitz–Ploem reflection contrast system as it was realized on a Diavert inverted microscope stand. Light from a mercury arc lamp (LS) is collimated by a collimation lens (not shown), and then penetrates a ring-shaped illuminating aperture (iA), which is projected to the back focal plane of the objective by a second collimating lens (not shown). By passing a polarizer (P) the light becomes linearly polarized. A field-limiting aperture (fA) is focused via the objective in the object plane. A semireflecting plate (RP) directs the beam to the objective lens (L) without any change in polarization. The light is projected on the object (O), where it has the intensity $I_O$. A quarter-wavelength plate (λ/4) with its slow axis 45° to the polarizer's direction causes circular polarization of the illuminating beam and linear polarization of the reflected beam ($I_R$), but with a 90° difference in the direction of polarization. Therefore, $I_R$ penetrates the analyzer (A) crossed to the polarizer. Light reflected from the lens surfaces (beam exemplified between the main paths) with unaltered polarization does not cross the analyzer. To simplify the diagram, only one part of the light beam penetrating the iA is followed. (Reproduced, with permission, from Bereiter-Hahn *et al.* (1979).)

light source (typically a mercury arc lamp HBO 100 or similar), filter to obtain monochromatic light, polarizing filter, central or ring-shaped diaphragm (optional) to increase contrast (for RIC), a semireflecting mirror, and an oil immersion objective with quarter-wavelength plate which can be rotated in front of the lens. The arrangement of the components and the ray paths is shown in Fig. 2.

The optimum device produced so far (but no longer commercially available) consists of a Diavert inverted research microscope (Leica, Wetzlar) equipped with a 100-W or 200-W mercury arc lamp, a polarizer, and a second collimating lens in the incident illuminator stand (Fig. 2). The system can be adapted to most of the common research microscopes equipped with epifluorescence. Prins *et al.* (1993) tested a variety of microscopes for their RIM performance (Table I).

Oil immersion polarization optics (free of internal tension) with magnifications between 40× and 100× are recommended. Immersion is essential to obtain good pictures of low-reflecting specimens. Tension-free optics are necessary to work with polarized light. If phase optics are used, the virtual size of the dark central part of the ring-shaped illuminating aperture should exceed the outer diameter of the phase ring (seen with an auxiliary eyepiece). Then the influence of the phase ring on the reflection contrast image is negligible. Combined phase-reflection optics allow an easy comparison of phase and RIC images of a cell simply by changing illuminating systems. Illuminating ring-shaped apertures can be prepared photographically on document film, taking pictures of black (india ink) rings of the desired geometry and enlarging the negatives onto another film with very steep gamma.

TABLE I

| Microscope | Objective[a] | Polarization block |
|---|---|---|
| Leica Aristoplan or Diaplan | 1 | Pol block (513734)[b] |
| Leitz Diavert or Orthoplan | 1 | Pol block (513791) |
| Nikon Optiphot or Labophot | 1 | IGS block MXA 20138 |
| Olympus BH2-RFCA | 1 | HM-IGS block (3284) |
| Zeiss Axioplan (*infinite optics*), Axiovert (inverted microscope) | 2 | IGS block (487960) UV-barrier filter (467860-9903) |

[a] (1) Leica NPL 50 × NA 1.00 oel imm kontr phaco 2 (559206), Leica NPL 100 × NA 1.30 oel imm kontr phaco 2 (559207), or Zeiss Antiflex-Neofluar 63 × NA 1.25 oil (421800). (2) Zeiss Antiflex Plan-Neofluar 63 × NA 1.25 oel ph3 (440469). In addition to these objectives and polarizing filters, light deflectors must be introduced to avoid reflections from the far surfaces of the specimen (see Section V).

[b] Ordering numbers in parentheses.

If quantitative evaluation is envisaged monochromatic light must be used for illumination. For living cells, orange or near-infrared light is recommended because short wavelengths (including green light) cause severe photodamage during prolonged illumination with strong intensities. The most favorable filter combination comprises a heat-reflecting filter, a UV-absorbing filter, and a long-pass filter with its edge at 580 nm (e.g., K580 from Schott) in combination with a mercury arc lamp. This lamp has a strong emission band at 589 nm. This band is easily selected by this cheap filter combination. Animal cells have negligible absorption in this spectral range (a cytochrome a absorption band at 614 nm is very weak). Near infrared is even less hazardous; however, electronic imaging systems are needed for visualization.

## B. SPECIFIC INSTRUMENTATION

### 1. Total Internal Reflection Fluorescence

Total internal reflection fluorescence (TIRF) is achieved by adaptation of Ambrose's surface contact microscope (see above) to fluorescence illumination. The cells are attached to a prism (the prism may be connected to a cover glass using a thin film of immersion oil); the angle of incidence can be varied by moving a mirror. In this case the illumination is coming from one side only, rather than being conical. The angle of total reflection characteristic for the glass/medium interface is chosen. At areas where molecular contacts are formed, the local difference in refractive indices is smaller, allowing the light to evanesce toward the specimen for a certain distance. This evanescent light can be used to excite fluorochromes and thus allows one to study specifically fluorescent molecules in close proximity to the reflecting interface. Variation of the angle of incidence provides the possibility to calculate the distance of the fluorochrome from the glass surface. For a review see Axelrod (1990); detailed theoretical guidelines have been developed by Gingell *et al.* (1987).

### 2. Integration of RIM in Confocal Laser-Scanning Microscopy

Most modern confocal laser-scanning microscopes allow a reflection image of the specimen to be obtained. In this case contrast problems are minimized because of the spotlike illumination and the confocal diaphragm in front of the photomultiplier. A further advantage of confocality is the possibility of optical sectioning, which is preserved also in the reflection mode. It is easier to apply and it gives a larger

viewing field. A broader range of objectives, including water immersion objectives, can be used. One system has been developed (Olympus with Lasertec 1LM11 confocal microscope) that allows study of fast movements at video rate (Vesely *et al.*, 1993). The main disadvantage of confocal laser-scanning microscopy reflection imaging lies in the lack of a clearly defined illuminating aperture (provided by the ring-shaped aperture); the whole angular spectrum contributes to image generation. As a consequence it is almost impossible to achieve quantitative data on topography, cell/glass distances, or refractive index of cytoplasm. These disadvantages can be overcome by decreasing the numerical aperture of the objectives, i.e., by an iris aperture at the back focal plane, restricting the illuminating beam down to almost normal incidence.

## III. Applications and Image Interpretation

The theoretical background of image interpretation has been developed by Gingell (1981), Gingell and Todd (1979), Beck and Bereiter-Hahn (1981), and Bereiter-Hahn *et al.* (1979). The two main fields of application of RIM are to study surface topography of cells and membrane dynamics and contrast enhancement of cells after various staining procedures.

### A. SURFACE TOPOGRAPHY AND MEMBRANE DYNAMICS

RIM is used to view cells in culture adhering to a plane glass surface. If it is assumed that the cytoplasm is optically homogeneous, three optical interfaces may occur (Fig. 1): glass/culture medium, medium/cell, cell/medium (two thin layers on top of the glass). In areas where the cells are intimately attached to the glass, the glass/medium interface is replaced by a glass/cytoplasm interface (one thin layer on the glass). Light beams reflected from the various interfaces may interfere with each other. The resulting intensities depend on the differences in optical path lengths and the RI at the boundaries. Sufficient coherence length of the illuminating light is a prerequisite which is fulfilled by high-pressure mercury lamps.

Thus the topography of both the cellular surfaces may be revealed by a typical pattern of interference fringes, that of the upper surface (the culture medium facing) and that of the lower cell surface (facing the glass surface). As far as interference fringes appear, an estimation of the distances can be made because the distance between adjacent constructive (bright line) and destructive (dark lines) interferences corresponds to a quarter wavelength (the phase difference between adjacent maxima and minima corresponds to $\lambda/2$, but the light must pass the layer twice before interfering). Therefore, the geometrical difference of layer thickness ($d$) between adjacent maxima and minima is given by

$$d = \lambda \cos \beta / 4n \tag{4}$$

where $d$ is the thickness of the layer between maxima and minima of adjacent interference fringes, $\lambda$ is the wavelength of light in a vacuum, $n$ is the refractive index of the layer, and $\beta$ is the angle of incidence of the illuminating beam (normal incidence: $\cos \beta = 1$).

Zones of close contact of the cells to the glass appear dark gray, *focal contacts* almost black. Their brightness does not change considerably by changing either the

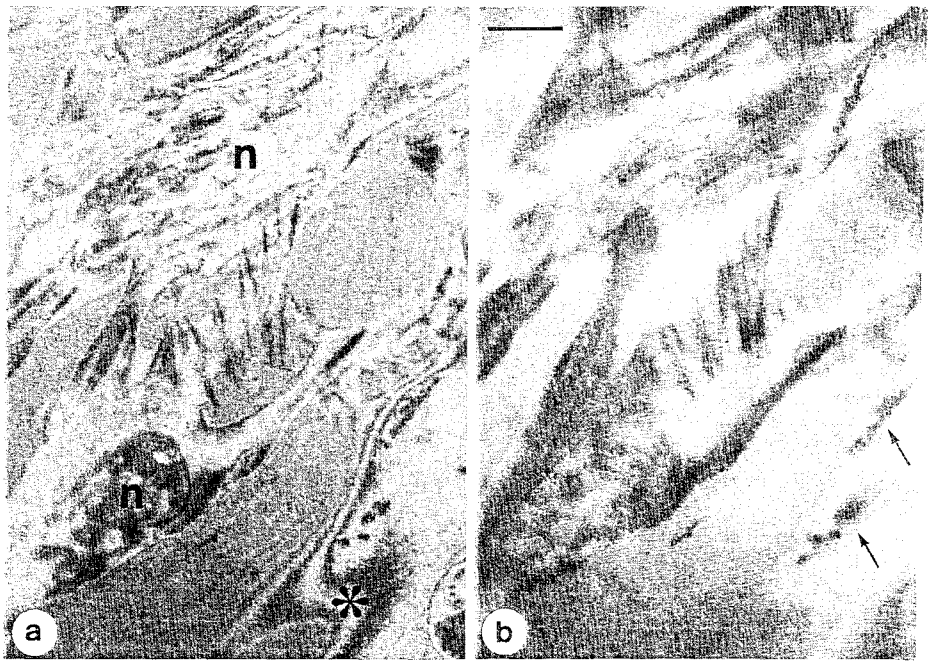


FIGURE 3 RIC images of living PtK2 cells attached to a glass slide viewed at diffe angles of conical illumination determined by a ring-shaped aperture: (a) 22° (mean angl incidence), (b) 40°. Diavert microscope, objective 100×. Bar = 10 μm. The appearanc those cell regions that are in molecular contact with the glass surface is almost the sam the two angles of incidence (i.e., focal contacts—arrows in a, spotlike contacts—arrow b). The gray values of all those zones that are further apart from the glass result f interferences. These change because of angle-dependent optical path differences. At the l angle of incidence we look more into the depth. The separation of the lower cell surface f the glass is indicated by interference fringes (asterisks in a). There appears to be less inte ence at higher angles of incidence (b); therefore the image appears clearer and which cell parts are over or under another cell can easily be seen. This relationship cannot be ded from image a. Asterisk in a marks an area where the cell distance to the glass increase Nucleus.

wavelength or the angle of illumination (Fig. 3). Calculations of the cell/glass tances from these intensity distributions (which can be quantified by photome are restricted to cells of known cortical cytoplasm refractive index. The uncerta of this value prohibits any accurate calculations of cell/glass distance based intensity measurements at a single wavelength. Evaluation is only possible in s of λ/4, where the phase difference can be directly recorded, or with a two-wavele system. The same applies to the determination of the refractive index of cytopl when the distance from the cell to the glass is not known (Bereiter-Hah *al.*, 1979).

RIM allows us to follow very small changes and differences in thickness of c plasmic lamellae (Beck and Bereiter-Hahn, 1981). For instance, at an angle of dence of 30° and orange light (589 nm) in cytoplasm with a refractive inde 1.4, a geometrical difference in cell thickness of 0.1 μm is sufficient for maxir interference contrast [from maximum brightness to a minimum (or vice ver Thus, very small deviations of boundaries in the $z$ axis are revealed by RIM 4). Good examples are the flickering movements of erythrocyte membranes o vivid activities at the surface of nuclei in living cells. This potential has not used adequately.

If cells are homogeneously attached to a glass surface, the upper cell surfac which relatively smooth and the angle of incidence is known, the volume o

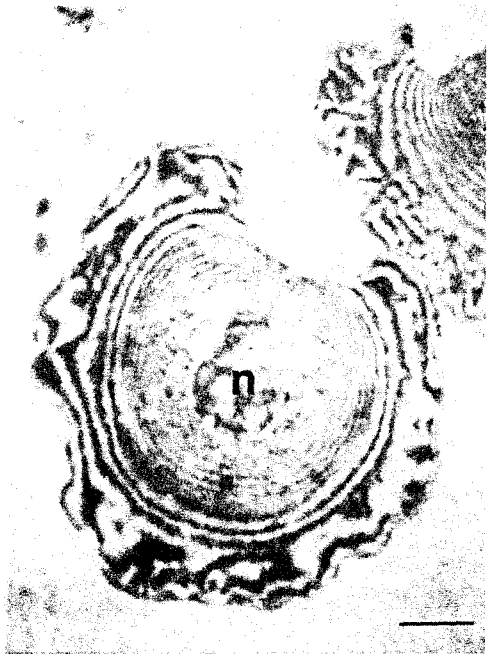


FIGURE 4 Single *Xenopus* tadpole epidermis cell in culture, viewed with RIC, objective 100×, mean angle of incidence 22°. These cells are closely attached to the glass; therefore the interference lines delineate the upper surface topography which is well resolved in the peripheral lamella. The concentric lines marking the cell body can be used to determine cell volume. For this purpose the focus should be slightly more toward the top of the cell. The bright spots close to the cell center are areas where the cells do not adhere properly. n, Nucleus. Bar = 10 $\mu$m. (Photograph courtesy of R. Strohmeier.)

cells can be determined using Eq. (4). The method works well with epithelial cells which normally fulfill the condition of smooth adherence to the glass. The upper cell surface is best revealed using an angle of incidence $0° \leq 22°$. The surface profile is delineated by the course of interference rings (Fig. 4). The cell volume comprises a stack of disks with a thickness equal to the thickness difference between the interference lines [according to Eq. (4)]. The areas delineated by each interference line are measured (e.g., using an interactive image analyzing system). Multiplication of the single areas by the thickness difference gives the volume of each of the "disks." The total of the "disk" volumes is the cell volume. For correct calculations the refractive index of the cytoplasm has to be known. This is of particular importance when osmotic volume changes are to be followed.

To determine the refractive index, the cells are immersed in solutions of different concentrations of bovine serum albumin in saline. The albumin content is varied by mixing two solutions of different concentrations, as is done for density centrifugation. The cells are viewed using a phase-contrast microscope and the BSA concentration is increased until the contrast of the cytoplasm disappears. At this point the refractive index of the immersion medium equals that of the cytoplasm. Then the refractive index of the medium can immediately be measured with an Abbé refractometer.

## B. CONTRAST ENHANCEMENT OF STAINED CELLS

Many stained biological specimens show an increase in contrast when viewed in reflected light. Membrane surfaces, chromosomes, and cytoskeletal elements have